

Arbitrary Mode Size Conversion with 3D-Nanoprinted Couplers: A Generic Coupling Strategy

Huiyu Huang¹, Zhitian Shi¹, Giuseppe Talli², Maxim Kuschnerov², Richard Pentyl¹,
Qixiang Cheng^{1,*}

¹Centre for Photonic Systems, Electrical Engineering Division, Department of Engineering, University of Cambridge, Cambridge CB3 0FA, U.K

²Huawei Technologies Duesseldorf GmbH, European Research Center, Riesstraße 25, 80992 Munich, Duesseldorf, Germany
Author e-mail address: qc223@cam.ac.uk

Abstract: We present a solution for efficient off-chip coupling with no requirement of on-chip mode engineering and additional manufacturing processes. A 10.4 μm to 4 μm fiber-to-chip mode-field-dimension conversion is demonstrated with $\sim 2\text{dB}$ loss across $>100\text{nm}$ wavelength range.

© 2024 The Author(s)

1. Introduction

Photonic integrated circuits are widely acknowledged as a game-changing technology driven by the needs of modern communications [1] and are enabling a host of innovations, including computing [2], sensing [3], imaging [4], etc. Off-chip coupling, however, is currently a major hurdle, especially for fiber-to-chip coupling, due to the large mode size mismatch. Many efforts have been made to develop dedicated mode size converters on different platforms, these usually involve additional processes such as substrate undercutting [5] or depositing secondary waveguides [6]. A generic solution that eliminates the need of on-chip mode engineering and additional manufacturing processes is thus much needed to break the “packaging bottleneck”.

In this work, we present a simple approach to off-chip coupling solution that can match the mode size over an ultra-large bandwidth range. The underlying mode-size conversion at an arbitrary ratio is accomplished by introducing parabolic micro-reflectors, the nature of optical reflection enabling it to be wavelength agnostic. By taking advantage of the additive 3D-nanoprinting manufacturing method, we demonstrate the proposed low-loss off-chip coupling strategy over an ultra-broad bandwidth, and more excitingly, with passive alignment capability. A Professional GT2 (Nanoscribe GmbH) system is used throughout this work [7]. We test the nano-printed couplers for high mechanical stability and high coupling efficiency using fiber-to-fiber coupling. We also demonstrate fiber-to-chip coupling that has a mode-field-dimension conversion ratio of as large as 250 % with a loss of as low as 2 dB/facet, almost perfectly agreeing to the simulation results.

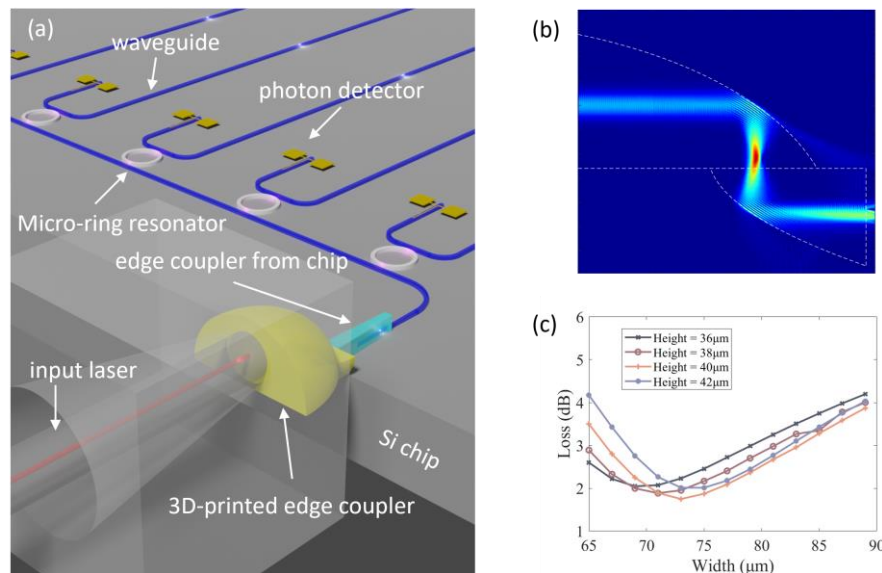


Fig. 1: (a) Schematic of the fiber-to-chip coupler (scale bar, 150 μm), (b) a simulated propagation profile in the reflector, and (c) geometry optimization for SMF28 to chip coupling with a silicon waveguide. Height and width stand for the geometry of the parabolic-shaped reflectors.

2. Modelling and Simulation

The reported 3D-nanoprinted edge coupler consists of a pair of parabolic-shaped reflectors and plug-in funnels, as shown in Fig.1a. The optical beam reflects twice at the resin/air interfaces, and then exits from the coupling unit and enters a second waveguide/fiber (Fig.1b). The shapes of the parabola are optimized to precisely determine the light propagation path inside the coupler. When the two parabolic reflectors are symmetrical in shape and size, the output mode field diameter (MFD) will remain unchanged. Altering the second mode reflector's dimensions changes the MFD of the output mode, achieving mode size conversion. In the following example, the geometry of reflectors is optimized using the Lumerical FDTD module to match the different modes of an SMF28 fiber and a silicon waveguide. The optimization results are shown in Fig.1c. During the free-space propagation, the light beam inevitably gets diverged and aberrated, which will compromise overall coupling efficiency. By altering the incident position of light, the aberration can be mitigated.

In addition to the optical components, a coupling frame fabricated on the chip plays a critical role as a guiding funnel in achieving passive alignment for input fibers. The geometric dimensions of the coupling cuboid frame measures $500\ \mu\text{m} \times 300\ \mu\text{m} \times 300\ \mu\text{m}$ and features a circular truncated cone truncation with an upper diameter of $130\ \mu\text{m}$ and a lower diameter of $250\ \mu\text{m}$ (see fig. 1a). This design is crafted to streamline the plug-in procedure and ensure precise alignment. Notably, the frame model extends into the chip edge by $20\ \mu\text{m}$, securing a snug fit between the resin frame and the chip edge post-printing. To further enhance the stability of the plug-in process, a $20\ \mu\text{m}$ bayonet is presented at the end of the truncated cone.

3. Fabrication

The parabolic-shaped couplers are fabricated using a direct laser writing system, Nanoscribe Professional GT2, which employs a $25\times$ objective lens in conjunction with IP-n162 resin, chosen for having the highest refractive index among the IP series offerings. Such a selection not only expedites the fabrication process but also ensures a high level of resolution and precision. For the fiber-to-fiber testing structures, the prototypes are printed onto a silica substrate coated with indium tin oxide (ITO). For fiber-to-chip testing structures, an on-chip printing technique was adopted, for the pivotal pre-printing alignment step. The test chip features a polymeric waveguide created with IP-n162 resin on a polymer base produced with IP-S resin. Notably, the IP-S base possesses a lower refractive index than the waveguide, facilitating signal mode propagation. The waveguide design aims for a MFD of $4\ \mu\text{m}$, closely resembling the mode size within silicon chips. Horizontal alignment is achieved using a visual monitoring system that utilizes a built-in camera within the Nanoscribe system. Meanwhile, the interface between the ITO-coated substrate and the base layer serves as the reference point for vertical alignment, leveraging the significant refractive index contrast. To optimize the printing process, different recipes are employed to minimize surface scattering and attain finely structured components with excellent surface smoothness, thus minimizing optical losses. To elaborate further, the mechanical and optical components are initially printed separately and later merged into a unified structure through manual coding of the printing file, thus reducing the process into a single step. In total, the entire printing procedure is completed in approximately 25 minutes, which can be further shortened by altering the printing recipe. A top-view optical microscope image of the printed structure (Fig.2) demonstrates the precision of alignment and control over surface roughness maintained throughout the entirety of the printing process.

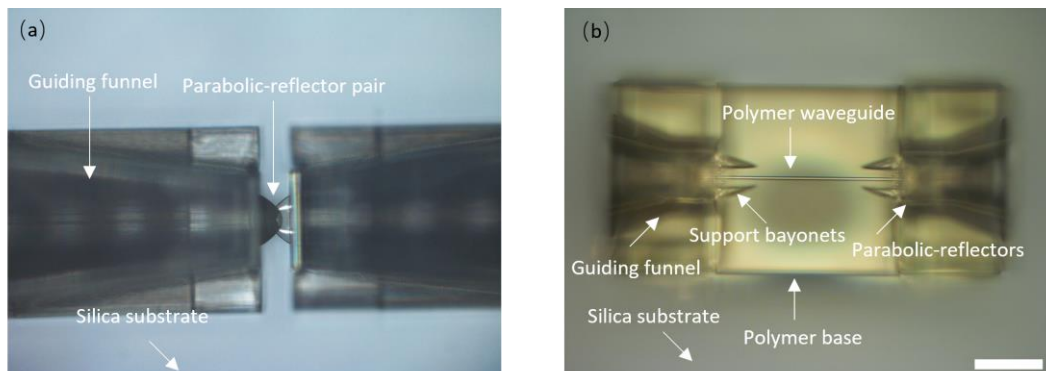


Fig. 2: (a) Printed fiber-to-fiber coupler under optic microscope, (b) Fiber-to-chip coupler under optic microscope (scale bar, $100\ \mu\text{m}$).

4. Characterization results

Four different designs are fabricated to match different MFD situations: SMF28 to SMF28; SMF28 to a high numerical aperture fiber (HNAF); SMF28 to an ultra-high numerical aperture fiber (UHNAF); and SMF28 to a polymer waveguide. The MFDs of SMF28, HNAF and UHNAF and the polymer waveguide at around 1550 nm are 10.5 μm , 6.9 μm , 4.8 μm and 4 μm , respectively. First, SMF28 (Thorlabs SMF-28-J9), HNAF (Thorlabs 980HP) and UHNAF (Thorlabs UHNA1) are cleaved and attached to a 3-axis optical stage (Thorlabs MAX312D). The light from a tunable laser (Thorlabs TLX1) is then guided into the SMF28 and propagates through the printed optical coupler into the second optical fiber (SMF28, HNAF or UHNAF) or polymer waveguide, and finally collected by an optical power meter. The fabricated structure is measured to have a loss of 0.8 dB for SMF28 to SMF28 coupling, 1.7 dB for SMF28 to HNAF coupling, 1.4 dB for SMF28 to UHNAF coupling, and 2.2 dB for SMF28 to chip coupling. The transmission over a broad wavelength ranging from 1500 nm to 1600 nm is plotted in Fig. 3 (measurement limited by the laser tuning range). The deformation in the 3D-nanoprinted structures during the curing process leads to a slightly higher loss, compared with the results acquired from the FDTD simulation, especially for those with smaller MFDs. This can be mitigated by further optimizing the mechanical structure.

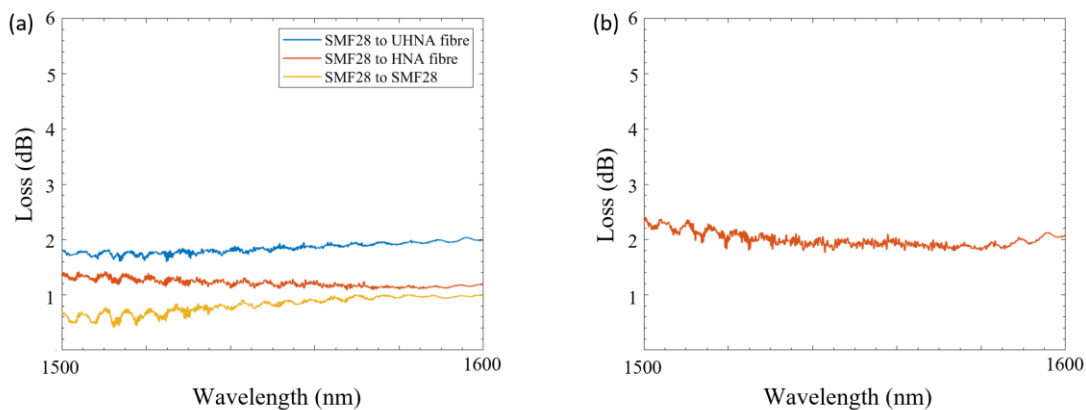


Fig. 3: Experimental results of (a) fiber-to-fiber coupling loss, SMF28 to SMF28, HNA and UHNA tested, and (b) fiber-to-chip coupling loss.

5. Conclusions

We propose and demonstrate a new hassle-free off-chip coupling solution that can arbitrarily convert the mode size over an ultra-large bandwidth range, with no need for additional fabrication processes. The parabolic-shaped micro-reflectors are fabricated using commercial 3D-nanoprinting equipment. Mechanical aligning funnels are also designed and attached to the reflectors to facilitate a fully-passive alignment process. A mode-field-dimension conversion ratio of as large as 250 %, from 10.4 μm to 4 μm MFD, is demonstrated with a loss of as low as 2 dB/facet over a broad bandwidth from 1500 nm to 1600 nm that is highly promising to tackle the off-chip “packaging bottleneck”.

- [1] K. Suzuki, R. Konoike, H. Matsuura, R. Matsumoto, T. Inoue, S. Namiki, H. Kawashima, and K. Ikeda, "Recent Advances in Large-scale Optical Switches Based on Silicon Photonics," in *Optical Fiber Communication Conference (OFC) 2022*, Technical Digest Series (Optica Publishing Group, 2022), W4B.6.
- [2] X. Yan, S. Gitt, B. Lin, D. Witt, M. Abdolahi, A. Afifi, A. Azem, A. Darcie, J. Wu, K. Awan, M. Mitchell, A. Pfenning, L. Chrostowski, and J. F. Young, "Silicon photonic quantum computing with spin qubits," *APL Photonics* **6**, 070901 (2021).
- [3] F. Gardes, A. Shooa, G. De Paoli, I. Skandalos, S. Ilie, T. Rutirawat, W. Talataisong, J. Faneca, V. Vitali, Y. Hou, T. D. Bucio, I. Zeimpekis, C. Lacava, and P. Petropoulos, "A Review of Capabilities and Scope for Hybrid Integration Offered by Silicon-Nitride-Based Photonic Integrated Circuits," in *Sensors*, (2022).
- [4] N. Dostart, B. Zhang, M. Brand, D. Feldkhun, M. Popović, and K. Wagner, "Fourier-basis structured illumination imaging with an array of integrated optical phased arrays," *J. Opt. Soc. Am. A* **38**, B19-B28 (2021).
- [5] D. Coenen, H. Oprins, Y. Ban, F. Ferraro, M. Pantouvaki, J. Van Campenhout, and I. De Wolf, "Thermal Modelling of Silicon Photonic Ring Modulator with Substrate Undercut," *J. Lightwave Technol.* **40**, 4357-4363 (2022).
- [6] Y. Maegami, R. Takei, E. Omoda, T. Amano, M. Okano, M. Mori, T. Kamei, and Y. Sakakibara, "Spot-size converter with a SiO₂ spacer layer between tapered Si and SiON waveguides for fiber-to-chip coupling," *Opt. Express* **23**, 21287-21295 (2015).
- [7] H. Huang, Z. Shi, J. Wei, C. Zhong, G. Talli, M. Kuschnerov, Q. Cheng, and R. Penty, "3D Nano-printed Coupler with Parabolic Reflectors," in *CLEO 2023*, Technical Digest Series (Optica Publishing Group, 2023), SF10.3.